

2627

~~CONFIDENTIAL~~

NRL Memorandum Report 2467

Cy 21

**The Microwave Emissivity of Foam
on a Water Surface**
[Unclassified Title]

LEE U. MARTIN

*Airborne Radar Branch
Radar Division*

August 1972



NAVAL RESEARCH LABORATORY
Washington, D.C.

~~CONFIDENTIAL~~

Downgraded at 12 year intervals;
Not automatically declassified.

Distribution limited to U.S. Government Agencies only; test and evaluation, August 1972. Other requests for this document must be referred to the Director, Naval Research Laboratory, Washington, D.C. 20390.

DDC - B (T4E)

CONTENTS

ABSTRACT	iii
PROBLEM STATUS	iii
AUTHORIZATION	iii
INTRODUCTION	1
THEORETICAL DISCUSSION	2
APPARATUS AND PROCEDURE	4
X-Band	5
K-Band	5
EXPERIMENTAL PROCEDURE	6
DATA REDUCTION	6
RESULTS - SKY AND CALM POOL	8
X-Band	8
K-Band	9
EVALUATION OF DATA	9
FOAM MEASUREMENTS	9
X-Band	9
K-Band	10
SUMMARY OF FOAM PROPERTIES	11
EVALUATION OF PROCEDURE	12
CONCLUSIONS	12
Ship Wakes	12
Sea State	13
RECOMMENDATIONS FOR FUTURE WORK	13

~~CONFIDENTIAL~~

[REDACTED]

APPENDIX A - Nadir Viewing Correction	15
APPENDIX B - Interference Effect on $\Delta\epsilon$ at X-Band	16
APPENDIX C - Calibration Effect on $\Delta\epsilon$ at K-Band	17
APPENDIX D - Sky Correction	18
APPENDIX E - Roughness Correction	19
REFERENCES	20

ABSTRACT

(C) The increase in the microwave emissivity of a foamy water surface over that of a smooth water surface for various viewing angles has been measured under controlled conditions. Measurements were made at frequencies of 8.35 and 19.35 GHz and for both horizontal and vertical polarizations. The change in emissivity, $\Delta\epsilon$, was less at 8.35 GHz than at 19.35 GHz for both polarizations. The angular variation of $\Delta\epsilon$ was smaller with horizontal polarization than with vertical polarization for the frequencies investigated. Experimental results are used to draw tentative conclusions about the detection of ship wakes with microwave radiometers.

PROBLEM STATUS

This is an interim report on one phase of the problem; work is continuing on this and other phases.

AUTHORIZATION

NRL Problem R02-67A
Project PM-16-40058CZW44150000

THE MICROWAVE EMISSIVITY
OF FOAM ON A WATER SURFACE

INTRODUCTION

(C) Detecting the change in the microwave thermal emission of the sea caused by the presence of a ship is being evaluated as a method for detecting ships. In the absence of a ship, the radiation from the sea is the sum of the thermal emission of the water itself and the reflection from the sea surface of the sky's radiation. Emission from the water has an intensity proportional to the product of the water temperature and an emissivity factor. The intensity of reflected sky radiation is proportional to the product of the radiometric temperature of that part of the sky reflected at the angle of observation and a reflectivity factor. Because the effective temperature of the sky is low in most of the microwave spectrum, except at very low elevation angles, the thermal radiation of the water is usually the dominant component of microwave emission from the sea's surface. The wake of a ship changes (usually raises) the emissivity of the water. The ship itself usually has a much lower emissivity than the water, depending on the deck configuration. Observations of the microwave thermal emissions from ship wakes indicate that the principal change in emissivity is caused by the foamy part of the wake.

(C) Since ship detection depends on the change in the sea's emission caused by the presence of the ship, knowledge of the emissivity of the sea background is important. Both theoretical and experimental evidence indicates that the emissivity of the sea will be a function of observing wavelength, polarization, observation angle, temperature, salinity and surface roughness. Surface roughness produces large changes in the emissivity of the sea. In general, rougher seas have greater emissivities, particularly when observed with horizontal polarization. To some extent this can be explained by the increase in the angle of observation caused by the wave slopes. For small waves, diffraction effects also enter the problem. However, foam and breaking waves greatly increase the emissivity, and are believed to account for much of the surface roughness effects, especially for very rough seas. Droppleman (1970), developed a theory of the microwave emission of foam which considers foam as an impedance matching layer between the air and the water surface. According to this theory, the emissivity approaches its maximum value of 1.0 for foam depths equal to the observing wavelength in foam.

(C) Ground based measurements by Williams (1969), and Edgerton et al. (1971) at Aerojet General indicate that the emissivity of foam is high and probably approaches a value of 1.0. These ground based observations have been confirmed by radiometric measurements made from the Argus Island Tower, Hollinger (1970), and by airborne measurements of rough seas by NASA personnel, Nordberg et al. (1971).

(C) Since the microwave emissivity of foam is important in determining the emissivity of ship wakes and the sea background, the changes in emissivity due to foam were measured under controlled conditions. Dr. J. P. Hollinger (NRL Space Sciences Division) was just beginning a program of measuring the emissivity of foam at 19.35 GHz when the radiometric ship detection effort began in the Airborne Radar Branch. Dr. Hollinger's interest is the remote sensing of sea conditions with a microwave radiometer. The Airborne Radar Branch assisted Dr. Hollinger in the 19.35 GHz measurements and made corresponding measurements at 8.35 GHz.

(C) The measurements were carried out by measuring, for both horizontal and vertical polarization, the emissivity at 8.35 and 19.35 GHz of foam generated in a six-foot diameter pool. Measurements were also made on the pool without foam, and of the angular variation of sky temperature.

THEORETICAL DISCUSSION

(U) The power received by a microwave radiometer may be given in terms of antenna temperature, which is related to the observed "brightness temperature" distribution. The antenna temperature may be written as:

$$T_a(\theta, \phi) = \frac{1}{4\pi} \int_{\Omega} T_{bp}(\theta, \phi) D(\theta, \phi) d\Omega \quad (1)$$

Where,

(θ, ϕ) = zenith and azimuth angles respectively

$T_a(\theta, \phi)$ = antenna temperature

$T_{bp}(\theta, \phi)$ = polarized brightness temperature

$D(\theta, \phi)$ = directive gain of antenna

$d\Omega$ = increment of solid angle

For surface based observations, (no atmospheric attenuation), the brightness temperature $T_{bp}(\theta, \phi)$ may be written as:

$$T_{bp}(\theta, \phi) = \epsilon_p(\theta, \phi) T_{sfc} + r_p(\theta, \phi) T_{sky}(\theta, \phi) \quad (2)$$

Where,

- $\epsilon_p(\theta, \phi)$ = polarized emissivity of surface
 T_{sfc} = thermodynamic temperature of surface
 $T_{sky}(\theta, \phi)$ = microwave temperature of sky
 $r_p(\theta, \phi)$ = polarized reflectivity of surface

The emissivity and reflectivity are related by:

$$r_p(\theta, \phi) = 1 - \epsilon_p(\theta, \phi) \quad (3)$$

Assuming azimuthal symmetry, equation (2) may be written as follows for a calm pool of water:

$$T_{wp}(\theta) = \epsilon_p(\theta) T_{sfc} + r_p(\theta) T_{sky}(\theta) \quad (4)$$

For a water surface covered with a uniform layer of foam, equation (2) may be written as:

$$T_{fp}(\theta) = \epsilon_f(\theta) T_{sfc} + r_f(\theta) T_{sky}(\theta) \quad (5)$$

Equations (4) and (5) may be combined to give the change in brightness temperature due to the presence of foam.

$$T_{fp}(\theta) - T_{wp}(\theta) = [\epsilon_f(\theta) - \epsilon_w(\theta)] T_{sfc} + [r_f(\theta) - r_w(\theta)] T_{sky}(\theta) \quad (6)$$

Equation (6) assumes that the water and foam are at the same temperature. In the experiment to be described, the amount of reflected sky viewed by the radiometers was restricted by screens to ± 30 degrees from zenith. Since the variation of sky temperature over this angular range is small, the sky temperatures may be assumed to be a constant.

$$T_{fp}(\theta) - T_{wp}(\theta) = [\epsilon_f(\theta) - \epsilon_w(\theta)] T_{sfc} + [r_f(\theta) - r_w(\theta)] T_{sky}(\theta) \quad (7)$$

But,

$$\epsilon_w(\theta) + r_w(\theta) = 1 \quad (8)$$

$$\epsilon_f(\theta) + r_f(\theta) = 1 \quad (9)$$

And,

$$r_f(\theta) - r_w(\theta) = -[\epsilon_f(\theta) - \epsilon_w(\theta)] \quad (10)$$

Or,

$$T_{fp}(\theta) - T_{wp}(\theta) = \Delta\epsilon(\theta) [T_w - T_{sky}(\theta)] \quad (11)$$

~~CONFIDENTIAL~~
Where,

$$\Delta \epsilon(\theta) = \epsilon_f(\theta) - \epsilon_w(\theta) \quad (12)$$

is the change in emissivity due to the presence of foam.

The combination of equations (4) and (5) give an expression for the temperature of a water surface partially covered with foam.

$$T_{mp}(\theta) = \frac{A_w}{A_b} [\epsilon_w(\theta) T_{sfc} + r_w(\theta) T_{sky}(\theta)] + \quad (13)$$

Where,

$$\frac{A_f}{A_b} [\epsilon_f(\theta) T_{sfc} + r_f(\theta) T_{sky}(\theta)]$$

A_w = area covered by water

A_f = area covered by foam

A_b = area of antenna beam on surface

And,

$$A_w + A_f = A_b$$

Upon combining terms, equation (13) becomes:

$$T_{mp}(\theta) = T_{wp}(\theta) + \frac{A_f}{A_b} [T_{fp}(\theta) - T_{wp}(\theta)] \quad (14)$$

Upon substituting equation (11) into (14), the temperature of a partially foam covered surface is given by:

$$T_{mp}(\theta) = T_{wp}(\theta) + \frac{A_f}{A_b} \Delta \epsilon(\theta) [T_{sfc} - T_{sky}(\theta)] \quad (15)$$

The change in emissivity due to the presence of foam is then:

$$\Delta \epsilon(\theta) = \left[\frac{T_{mp}(\theta) - T_{wp}(\theta)}{T_{sfc} - T_{sky}(\theta)} \right] \frac{A_b}{A_f} \quad (16)$$

(U) The measurements of $\Delta \epsilon$ were made under controlled conditions by conducting the experiment in a 6 foot wading pool. This permitted the comparison of calm pool observations and of various depths of foam by varying the flow of air through the foam generator. Measurements were taken for various viewing angles and for horizontal and vertical polarization to determine the variation of $\Delta \epsilon$ as a function of foam depth, viewing angle and polarization.

APPARATUS AND PROCEDURE

(U) A block diagram of the radiometers used in this experiment is shown in Fig. 1. The radiometers, which operated at 8.35 and 19.35 GHz, were Dicke type with superheterodyne receivers which accepted

both sidebands. The receivers were switched between their horn-lens antennas and reference loads which were at a temperature slightly above ambient. Calibration was provided by argon noise sources coupled into the systems. When they were switched on, they added a known calibration temperature to the antenna temperature. A summary of the important parameters of the radiometers is given in Table 1.

TABLE 1

	<u>X-Band</u>	<u>K-Band</u>
Radiometer Type	Dicke, double-sideband superheterodyne receivers	
Antennas	Horn lens	Horn lens
Polarization	Horizontal or vertical	
Beamwidth	7° at 3 db	7° at 3 db
IF Bandwidth	240 MHz	300 MHz
Calibration	Argon noise source	
Integration Time	0.8 sec	1.0 sec
Noise Figure	11 db	9 db
Sensitivity (rms)	0.6°K	0.4°K

X-Band

(U)Figure 2 portrays the experimental arrangement for the X-band measurements. The radiometer was mounted on a fiberglass boom whose angle from the vertical could be adjusted. The distance of the radiometer along the boom, as well as the angle of the radiometer relative to the boom could each be adjusted. These adjustments were made so that the radiometer was always slightly farther from the pool surface than the nominal far field distance $2w^2/\lambda$, where w equals the antenna aperture size and λ is the observing wavelength.

K-Band

(U)Figure 3 portrays the experimental arrangement for the K-Band measurements. The radiometer was mounted on a support structure which could be moved relative to the pool. By varying the distance of the support from the pool, and by varying the angle of the radiometer, various viewing angles to the center of the pool could be obtained. The distance from the antenna to the pool surface exceeded $2w^2/\lambda$.

~~CONFIDENTIAL~~

(U)The pool, six feet in diameter, was filled with approximately a foot of water. The salinity was increased to that of sea water (35‰) by the addition of calcium chloride.

(U)The foam generator, shown in Fig. 4, consisted of a spiral of copper tubing with aquarium aerators attached at intervals. It was connected to the laboratory air supply from which various flow rates could be obtained. The input flow was monitored with a sensitive flow meter so that repeatable air flows could be obtained. A typical foam pattern at a flow rate of 6 ft³/min is shown in Fig. 5.

EXPERIMENTAL PROCEDURE

(U)For a typical measurement, the following procedure was followed:

1. The zero scale deflection was determined.
2. The reference load temperature was recorded.
3. The radiometric sky temperature was measured.
4. The radiometric sky temperature was measured with the argon noise source turned on.
5. Step 3 was repeated.
6. The radiometric temperature of the calm pool was measured.
7. The radiometric temperature of the foam at three flow rates was measured.
8. The radiometric temperature of the calm pool was measured with the argon noise source turned on.
9. Step 6 was repeated.
10. Step 2 was repeated.

(U)This procedure was carried out for five angles from nadir to 40 degrees from nadir. The polarization was then changed by rotating the antenna and the measurements were repeated. Auxiliary measurements of water temperature, dry and wet bulb temperatures and a visual estimate of sky conditions were recorded throughout the period of observation. The measurements which were made on two different days were compared for consistency.

DATA REDUCTION

(U) A section of the strip-chart record taken during the measurements at X-band for horizontal polarization and a viewing angle of 25 de-

grees, is shown in Fig. 6. This type of data was reduced using the following procedure.

1. The magnitude of the deflections were determined from the zero deflection line on the chart.
2. The antenna temperature was then calculated from the relation:

$$T_m = T_{ref} - \frac{T_{argon}}{X_{argon}} X \quad (17)$$

Where,

T_{ref} = reference load temperature ($^{\circ}$ K).

T_{argon} = argon noise temperature ($^{\circ}$ K).

X_{argon} = scale deflection of argon noise source.

X = scale deflection of (sky/pool) measurements.

The antenna temperature was then corrected for system losses by:

$$T_{ant} = L T_m - (L-1) T_{amb} \quad (18)$$

Where,

L = system loss ($L \geq 1$)

T_{amb} = ambient temperature ($^{\circ}$ K)

(U) The argon noise temperature had been determined previously by standard techniques to be 103° K. The system losses were determined by calibrating against the zenith sky using a standard gain horn and comparing this temperature to the observed sky temperature. The total loss determined in this manner was 0.6 db.

(U) The deflections caused by the argon noise source were slightly different for the sky and pool measurements, indicating that the deflections were non-linear. Accordingly, the average of the sky and pool values was used for the sky measurements while the pool value was used for the calm pool and foam measurements.

(U) For the K-band measurements, the argon noise temperature and system losses were unknown, so approximate values of these parameters were determined from the observed sky temperature in the following manner.

(U) An extensive study by Mango (1971) has indicated a good correlation between surface absolute humidity and observed sky temperature. Thus, the absolute humidity was calculated from the wet and dry bulb temperatures. Then, the true sky temperatures were determined for the

angles of interest. Upon combining equations(17) and(18):

$$T_{ant} = T_{amb} + L (T_{ref} - T_{amb}) - \frac{L T_{argon} X}{X_{argon}} \quad (19)$$

Knowing the true sky temperature, the deflection caused by the argon noise source and the ambient temperature, a plot of loss versus argon noise source temperature could be made. This plot provides a range of values which satisfy equation (19). The average values of these parameters, $T_{argon} = 106^{\circ}\text{K}$ and Loss = 0.048 db were chosen. After these values were determined, the analysis was identical to the procedure used for the X-band measurements.

RESULTS - SKY AND CALM POOL

X-Band

(U) Figures 7-10 show the observed values of the radiometric temperatures as a function of angle for the calm pool and sky for both polarizations, and for the two days of measurements. Figure 11 shows all sky temperature measurements, including both polarizations. For the calm pool data, a theoretical curve, based on the water temperature and salinity, is shown for comparison. The data are given in terms of antenna temperature, since the detailed antenna pattern and efficiency are unknown. The following results can be seen from the curves:

(U)1. Figures 7-10 show sky temperatures are consistent for both polarizations and for both days of observations. This is to be expected because the atmosphere is randomly polarized and meteorological conditions were similar on both days. The sky temperature increases as the secant of the observation angle as expected, although the magnitude is consistently too high compared to theory. The explanation for this is unknown, although the support-beam may be influencing the observations.

(U)2. For the calm pool data there is good agreement with theory for vertical polarization (Figs. 7 and 9) except at the nadir. For horizontal polarization (Figs. 8 and 10), the angular variation has the expected form, except for angles of nadir and 40 degrees. However, the temperatures are larger than expected, especially on 21 January. Since interference (RFI) was observed on a monitoring scope before the first days data was taken, this is the most likely explanation for the discrepancy. The high radiometric temperatures observed at nadir for both polarizations are probably caused by the reflection of the antenna's thermal emissions from the smooth water and back into the antenna again. Calculations made of the expected magnitude of the effect (see Appendix A) come close to the observed values.

K-Band

(U) Figure 12 shows the observed values of the angular variation of the radiometric temperatures of the calm pool for both horizontal and vertical polarizations. Sky temperatures are not shown because data were taken only at $\theta=40$ degrees. The agreement between theory and the observed values is good, with the greatest difference of about 5% being observed for vertical polarization. Since the observed temperatures depend upon the approximated values of noise source temperature and system loss, a check was made of the other possible values of these parameters which satisfy Eq. (19). They gave closer agreement for horizontal polarization but only a slight improvement for vertical polarization.

EVALUATION OF DATA

(U) The agreement between theory and the observed values of radiometric temperatures for the calm pool and the sky are good, considering the RFI problems at X-band and the difficulties of calibration at K-band. The angular variations agree with theory and the measurements are consistent. Some of the disagreement with theory may be due to the antenna pattern characteristics and possible side-lobe corrections which should be applied to the data.

FOAM MEASUREMENTS

X-Band

(U) The increase in emissivity due to foam, $\Delta\epsilon$, may be measured as the difference in antenna temperature between the foam covered and the calm pool. There is some evidence of interference in the horizontally polarized calm pool data, and the value of $\Delta\epsilon$ could be affected if the interference was different when measurements were made on the calm pool and when they were made on the foam covered pool. Since the values of $\Delta\epsilon$ for both days and both polarizations were comparable, it was assumed that the effects of interference on the calm pool measurements were similar to the effects on the measurements on the covered pool. It is shown in Appendix B that this assumption, along with equation 16, leads to $\Delta\epsilon$ being independent of interference if true sky temperatures values are used in the calculations.

(U) From photographs taken of the foam coverage for various air flow rates, the percent of the surface of the pool covered by foam was determined. For the X-band measurements, the coverage ranged from 52% for the measurements at the nadir to 54% at 40 degrees viewing angle with no significant difference between the air flow rates.

(U) Figures 13-16 show $\Delta\epsilon$ versus viewing angle for the various flow rates, for both horizontal and vertical polarizations and for both days of observations. The following features should be noted:

- ~~CONFIDENTIAL~~
- 1) Figures 13-16 show the value of $\Delta\epsilon$ is less than 0.6, meaning that the foam was not a perfect absorber.
 - 2) The angular variation of $\Delta\epsilon$ for horizontal polarization is small, (Figs. 13 & 15), and less than for vertical polarization (Figs. 14 & 16).
 - 3) Figures 13-16 show that the magnitude of $\Delta\epsilon$ increases with increasing flow rate (i.e. depth of foam) for a specific angle.
 - 4) By comparing Figs. (13 & 14) and (15 & 16), the depth of foam determines whether horizontal or vertical polarization will give a larger change in $\Delta\epsilon$.

K-Band

(U) For the K-band measurements, the percentage of the beam covered by foam ranged from 55% at vertical incidence to 60% at 40 degrees. Because of the lack of a good calibration, an attempt was made to determine what effect the calibration had on $\Delta\epsilon$ values. It is shown in Appendix C that for the conditions of this experiment, $\Delta\epsilon$ can be written as:

$$\Delta\epsilon(\theta) = \left[\frac{X_{pool} - X_m}{X_{sky}} \right] \frac{A_b}{A_f} \quad (20)$$

Where,

X_{pool} = deflection for the calm pool,

X_m = deflection for foam covered pool,

X_s = deflection for sky measurement,

and the other terms have been defined previously.

(U)Equation (20) is independent of the noise source temperature and system losses. A minor difficulty arises in that the sky deflection should be at the corresponding angle of observation. Since sky measurements were made only at zenith angles of 40 degrees, a method of correcting the sky deflections is given in Appendix D.

Figures 17 and 18 show the values of $\Delta\epsilon$ for horizontal and vertical polarization as a function of observing angle and for various flow rates. Several features to be noted are the following:

- 1) There is little difference between the two polarizations, particularly at the lower viewing angles.
- 2) There is less angular variation of $\Delta\epsilon$ for horizontal polarization than for vertical polarization.

- 3) $\Delta\epsilon$ increases with increasing flow rate to the maximum possible, implying the emissivity of foam approaches unity.

(U)A point which must be mentioned in regard to the above features is the possible effect of surface roughness. The "clear areas" in the foam tank were assumed to be smooth water. If this assumption is not true, it is shown in Appendix E that a correction term should be applied. This correction term is:

$$\Delta\epsilon' = \frac{A_w}{A_f} \tag{21}$$

Where,

$\Delta\epsilon'$ = the emissivity change due to roughness

A_w = the area covered by water.

A_f = the area covered by foam.

This term should:

- 1) increase with flow rate because the water is more turbulent.
- 2) be larger for horizontal than for vertical polarization.
- 3) increase with angle for horizontal polarization and decrease with angle for vertical polarization.

The magnitude of the correction is unknown, although it might be as large as several percent. However, it is a factor which must be taken into account, and may modify the features of the $\Delta\epsilon$ curves for K-band. Hopefully this factor can be eliminated in future measurements.

SUMMARY OF FOAM PROPERTIES

(U)The following tentative conclusions are drawn from the experimental measurements.

- 1) The change in emissivity ($\Delta\epsilon$) increases with depth of foam up to at least 1.5 cm for both frequencies.
- 2) The angular variation of $\Delta\epsilon$ is small, being less for horizontal polarization than for vertical polarization and less at X-band than at K-band.
- 3) At X-band, $\Delta\epsilon$ can be greater at either horizontal or vertical polarization, depending on the depth of foam.
- 4) For foam depths less than 1.5 cm, $\Delta\epsilon$ is greater at K-band than at X-band for the same depth of foam and viewing angle.

[REDACTED]

EVALUATION OF PROCEDURE

(U) Several features of the experiment need to be mentioned.

- 1) The lack of foam coverage over the beam caused $\Delta\epsilon$ to be inversely proportional to the area covered by the foam. Since foam coverage was only about 50%, a large correction was applied to obtain the $\Delta\epsilon$ values.
- 2) The non-foam areas of the pool were assumed to be smooth water. The photographs of the surface indicate that there was foam and surface roughness in these "clear" areas, but the magnitude of these effects are unknown.
- 3) The photographs show that the foam tended to pile up in the foamy areas and that in some areas of the pool, the bubbles were larger than in other areas. Over the area of the beam these effects were probably small, but under specific circumstances, they could be important.
- 4) As the foam becomes older, more and more of the liquid drains from it and hence changes its water content and emissivity. Under these conditions there will be a gradient of water content from the bottom to the top of the foam layer and a lower effective emissivity for the foam layer as a whole.

CONCLUSIONS

SHIP WAKES

(C) Based on the data from this experiment, some tentative conclusions may be drawn about the possible detection of ship wakes with microwave radiometers.

- 1) The increase in brightness temperature above the sea background will increase with frequency (approaching $\Delta\epsilon \approx 0.6$) for foam depths less than the observing wave length in foam. For greater foam depths, the longer wave lengths will give a greater increase in signal.
- 2) The magnitude of the foam generated signal above the background should show very little angular variation, neglecting atmospheric effects. However, when making observations from above the surface, atmospheric effects must be taken into consideration.

- [REDACTED]
- 3) The experiment showed that the increase in temperature over the calm pool caused by the foam was only a little different for horizontal and vertical polarizations. Over the open ocean where roughness effects are greater at horizontal polarization, the increase would then be greater for vertical polarization.

SEA STATE

(C) The effect of background sea state will influence the possibility of ship detection in two possible ways. The first is changes in surface roughness from point to point. A one percent change in the temperature increase due to roughness over the beam area will provide a change in signal about equal in magnitude to that expected from a diluted ship wake. Since roughness changes increase with frequency and are greater for horizontal than vertical polarization, background roughness effects can be reduced by going to as low a frequency as possible and to vertical polarization.

(C) The second effect of the background sea will be the natural foam on the sea surface which appears at sufficient surface wind speeds. This background foam will increase the observed brightness temperature directly proportional to its areal coverage, weighted by the antenna pattern. Under some conditions, this might completely mask the ship wake. A method of solution would be to compare sequential data points, but if the point to point variation in foam coverage is greater than the increase due to the ship wake, then other methods of separating the background foam from the ship wake must be found.

RECOMMENDATIONS FOR FUTURE WORK

(U) Future investigations into the properties of foam should include the following:

- 1) Complete uniform foam coverage of the beam or accurate knowledge of the foam coverage.
- 2) A sufficiently stable foam so that the air flow can be turned off and possible roughness effects eliminated.
- 3) Foam measurements should be extended to other frequencies.
- 4) For a specific frequency, the following foam properties should be determined:
 - a) the emissivity of foam as a function of foam depth.

- 
- b) the influence of bubble size on the foam emissivity.
- c) the water content of the foam and the range of values for various bubble sizes and contaminants in the water.
- d) the effect of drainage on foam emissivity and its dependence on the thickness of the foam layer and contaminants in the water.
- 

~~CONFIDENTIAL~~

APPENDIX A - NADIR VIEWING CORRECTION

(U) For nadir viewing, the physical setup was as in Fig. 2 of the text.

(U) The temperature increase, ΔT , due to the antenna's reflection in a calm water surface, and assuming the sky temperature is zero, may be written as:

$$\Delta T = \frac{\Omega_a}{\Omega_b} \times T_b \times r_w \quad (A1)$$

Where:

Ω_a = solid angle of the reflected antenna aperture

Ω_b = solid angle of antenna beam

T_b = brightness temperature of aperture

r_w = reflectivity of water surface

The effective size of the antenna aperture is given by

$$A_a = G\lambda^2/4\pi \quad (A2)$$

Where:

G = gain of the antenna

λ = wavelength

Now

$$G \approx 3 \times 10^4 / \theta^2 \quad (A3)$$

Where θ equals the half-power beamwidth in degrees. Combining the two preceding equations, one can write

$$A_a = 3 \times 10^4 \lambda^2 / \theta^2 4\pi \quad (A4)$$

The area of the antenna beam can be written as

$$A_b = \pi r^2 = \pi (h \tan \theta/2)^2 \quad (A5)$$

Where h equals twice the distance from the antenna to the pool surface. Substituting in values for the parameters, one obtains

$$\frac{\Omega_a}{\Omega_b} = A_a/A_b = 3 \times 10^4 \lambda^2 / 4\pi^2 \theta^2 (h \tan \theta/2)^2 = .064 \quad (A6)$$

And ΔT then becomes

$$\Delta T = .064 \times 278^\circ K \times 0.62 = 11.1^\circ K \quad (A7)$$

(U) For the measurements made with foam present, the reflectivity in the backscattering direction is unknown and will be neglected. Thus, the calm pool data have been corrected by 11°K before $\Delta\epsilon$ was calculated.

APPENDIX B - INTERFERENCE EFFECT ON $\Delta\epsilon$ AT X-BAND

(U) Since the data of the calm and foamy pools were averaged over at least a minute and the temperature differences between the foamy and calm pool were comparable on the two days of measurement, it was assumed that the interference was constant between the calm pool and foam measurements. However, since several minutes passed between the sky and pool measurements, the interference was assumed to be different between the sky and pool data. With these assumptions,

$$T_{\text{pool obs}} = T_{\text{pool true}} + \psi \quad (B1)$$

$$T_{\text{m obs}} = T_{\text{m true}} + \psi \quad (B2)$$

$$T_{\text{sky obs}} = T_{\text{sky true}} + \psi' \quad (B3)$$

Where ψ equals interference and $\psi \neq \psi'$

Substituting these expressions into Eq. (16),

$$\Delta\epsilon_{\text{true}} = \left[\frac{T_{\text{m obs}} - \psi - T_{\text{pool obs}} + \psi}{T_{\text{sfc}} - T_{\text{sky obs}} - \psi'} \right] \frac{A_b}{A_f} \quad (B4)$$

Or

$$\Delta\epsilon_{\text{true}} = \left[\frac{T_{\text{m obs}} - T_{\text{pool obs}}}{T_{\text{sfc}} - T_{\text{sky obs}} - \psi'} \right] \frac{A_b}{A_f} \quad (B5)$$

$\Delta\epsilon$ is only dependent on the sky interference. Either corrected sky values or the true sky values may be used. Either way the correction is small because $T_{\text{sfc}} \gg T_{\text{sky}}$. In the data analysis, the true sky values were used as determined from the standard gain horn. Even if the interference was different between the calm pool and foam measurements, $\Delta\epsilon$ would become

$$\Delta\epsilon_{\text{true}} = \left[\frac{T_{\text{m obs}} - T_{\text{pool obs}}}{T_{\text{sfc}} - T_{\text{sky true}}} \right] \frac{A_b}{A_f} + \left[\frac{\psi_{\text{foam}} - \psi_{\text{pool}}}{T_{\text{sfc}} - T_{\text{sky true}}} \right] \frac{A_b}{A_f} \quad (B6)$$

and the total error would again be small.

CONFIDENTIAL

APPENDIX C - CALIBRATION EFFECT ON $\Delta\epsilon$ AT K-BAND

(U) Combining Eqs. (17) and (18), the antenna temperature can be written as,

$$T_{ant} = T_{amb} + L(T_{ref} - T_{amb}) - L \times T_{argon} \times X_{obs}/X_{argon} \quad (C1)$$

Or

$$T_{ant} = \alpha_1 - \alpha_2 X_{obs} \quad (C2)$$

Where

$$\alpha_1 = T_{amb} + L(T_{ref} - T_{amb}) \quad (C3)$$

$$\alpha_2 = L \times T_{argon} \quad (C4)$$

Substituting T_{ant} into Eq. (16),

$$\Delta\epsilon = \left[\frac{\alpha_1 - \alpha_2 X_{foam} - \alpha_1 + \alpha_2 X_{pool}}{T_{sfc} - \alpha_1 + \alpha_2 X_{sky}} \right] \frac{A_b}{A_f} \quad (C5)$$

Or

$$\Delta\epsilon = \left[\frac{\alpha_2 (X_{pool} - X_{foam})}{T_{sfc} - \alpha_1 + \alpha_2 X_{sky}} \right] \frac{A_b}{A_f} \quad (C6)$$

Now

$$T_{sfc} - \alpha_1 = T_{sfc} - T_{amb} - L(T_{ref} - T_{amb}) \quad (C7)$$

For the K_u band measurements,

$$T_{sfc} = 283^\circ K$$

$$T_{ref} = 293^\circ K$$

$$T_{amb} = 9^\circ C = 282^\circ K$$

Thus,

$$T_{sfc} - \alpha_1 = 1^\circ K + 1.01 \times 11^\circ K \approx 12.6^\circ K \quad (C8)$$

Since

$$\alpha_2 X_{sky} \approx 265^\circ K \quad (C9)$$

$(T_{sfc} - \alpha_1)$ may be neglected in comparison to $\alpha_2 X_{sky}$ with about a 4% error.

Thus,

~~CONFIDENTIAL~~

$$\Delta\epsilon \approx \frac{\alpha_2 (X_{pool} - X_{foam})}{\alpha_2 X_{sky}} \times \frac{A_b}{A_f} \quad (C10)$$

Or

$$\Delta\epsilon \approx \frac{X_{pool} - X_{foamy}}{X_{sky}} \frac{A_b}{A_f} \quad (C11)$$

The sky deflection must be at the angle of observation of T_p and T_f . Since this was not done during the observations, a correction factor was applied. The method is developed in Appendix D.

APPENDIX D - SKY CORRECTION

(U) For the K_u band measurements, the sky temperature was always measured at an angle of 40 degrees from zenith, while to determine $\Delta\epsilon$, the temperature of the sky at the angle of observation is required. To obtain the required sky temperature, one can correct the sky temperature at 40 degrees in the following manner. For a horizontally stratified atmosphere and up to moderate zenith angles, the sky temperature at zenith angle θ can be written as

$$T_{sky}(\theta) = T_m (1 - \exp^{-\alpha_0 \sec \theta}) \quad (D1)$$

Where

- T_m = mean radiating temperature of the atmosphere
- α_0 = zenith absorption in nepers

Or, if $\alpha_0 \sec \theta$ is small, which is true for our case,

$$T_{sky}(\theta) = T_m \alpha_0 \sec \theta \quad (D2)$$

Or,

$$T_{sky}(\theta) = \left(\frac{\cos 40^\circ}{\cos \theta} \right) T_{sky}(40^\circ) \quad (D3)$$

From Appendix C,

$$T_{sky}(\theta) = \alpha_1 - \alpha_2 X_{sky}(\theta) \quad (D4)$$

$$T_{sky}(40^\circ) = \alpha_1 - \alpha_2 X_{sky}(40^\circ) \quad (D5)$$

Or,

$$X_{sky}(\theta) = \frac{\alpha_1}{\alpha_2} \left(1 - \frac{\cos 40^\circ}{\cos \theta} \right) + X_{sky}(40^\circ) \frac{\cos 40^\circ}{\cos \theta} \quad (D6)$$

~~CONFIDENTIAL~~

Now,

$$\frac{\alpha_1}{\alpha_2} = \frac{T_{amb} + L(T_{ref} - T_{amb})}{L T_{argon} / \chi_{argon}} \quad (D7)$$

Using the values for T_{argon} and L that were determined previously,

$$\frac{\alpha_1}{\alpha_2} \approx 9.9 \quad (D8)$$

This value was then used with the observed data to correct the sky temperatures before $\Delta\epsilon$ was calculated.

APPENDIX E - ROUGHNESS CORRECTION

Assume that because of surface roughness, the emissivity is increased by a factor $\Delta\epsilon'$. Equation (13) then becomes

$$T_m = \left[\frac{A_w}{A_b} (\epsilon_w + \Delta\epsilon') T_{sfc} + (\gamma_w - \Delta\epsilon') T_{sky} \right] \quad (E1)$$

Or upon rearranging terms,

$$T_m = T_{pool} + \frac{A_f}{A_b} [T_{foam} - T_{pool}] + \left(1 - \frac{A_f}{A_b}\right) \Delta\epsilon' (T_{sfc} - T_{sky}) \quad (E2)$$

Now, from Eq. (11)

$$T_{foam} - T_{pool} = \Delta\epsilon_{true} (T_{sfc} - T_{sky}) \quad (E3)$$

And upon substituting Eq. (11) for $(T_f - T_p)$, one can write

$$T_m = T_{pool} + \frac{A_f}{A_b} \Delta\epsilon_{true} (T_{sfc} - T_{sky}) + \left(1 - \frac{A_f}{A_b}\right) \Delta\epsilon' (T_{sfc} - T_{sky}) \quad (E4)$$

Or,

$$\Delta\epsilon_{true} = \left[\frac{T_m - T_{pool}}{T_{sfc} - T_{sky}} \right] \times \frac{A_b}{A_f} - \frac{A_w}{A_f} \Delta\epsilon' \quad (E5)$$

Thus, to obtain the true $\Delta\epsilon$, a correction term must be subtracted from the observed $\Delta\epsilon$.

CONFIDENTIAL

REFERENCES (U)

1. Edgerton, A. T., F. Ruskey, D. Williams, A. Stogryn, G. Poe, D. Meeks, O. Russell, Microwave emission characteristics of natural materials and the environment, Final Tech. Rept. 9016R-3, Microwave Div., Aerojet-General Corp., El Monte, California, February, 1971.
2. Dippleman, J. D., Apparent microwave emissivity of sea foam, J. Geophys. Res., 75, 696-698, January, 1971.
3. Hollinger, J. P., Passive microwave measurements of the sea surface, J. Geophys. Res., 75, 5209-5213, September, 1970.
4. Mango, S. A., Measurements of atmospheric attenuation at 19.4 GHz and their relationship to the atmospheric water vapor content, Preprint, E. O. Hulburt Center for Space Research, Naval Research Laboratory, Washington, D. C., January, 1971.
5. Nordberg, W., J. Conaway, D. B. Ross, T. Wilheit, Measurements of microwave emission from a foam-covered, wind-driven sea, J. of Atmos. Sci. 28(3), 429-435, April, 1971.
6. Williams, G. F., Microwave radiometry of the ocean and the possibility of marine wind velocity determination from satellite observations, J. Geophys. Res., 74(18), 4591-459, 1969.

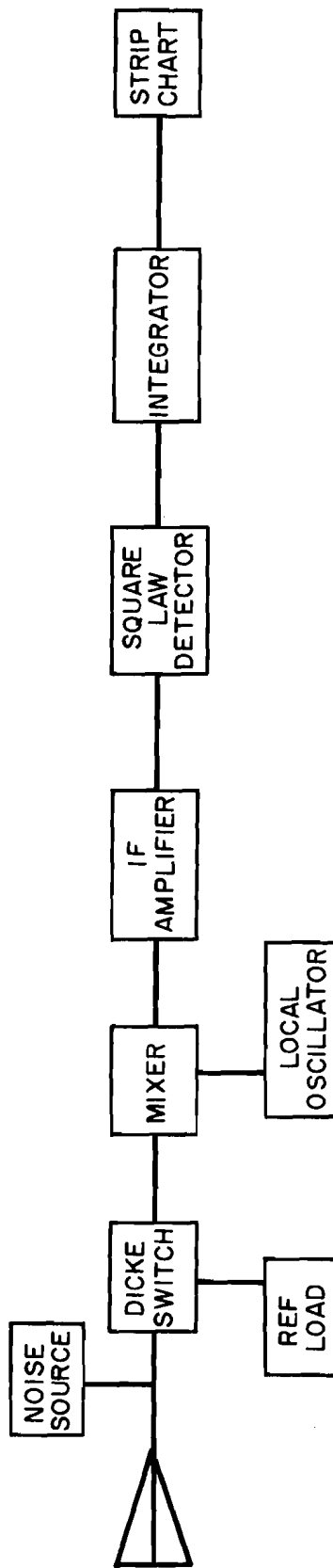


Fig. 1 - Block diagram of radiometers.

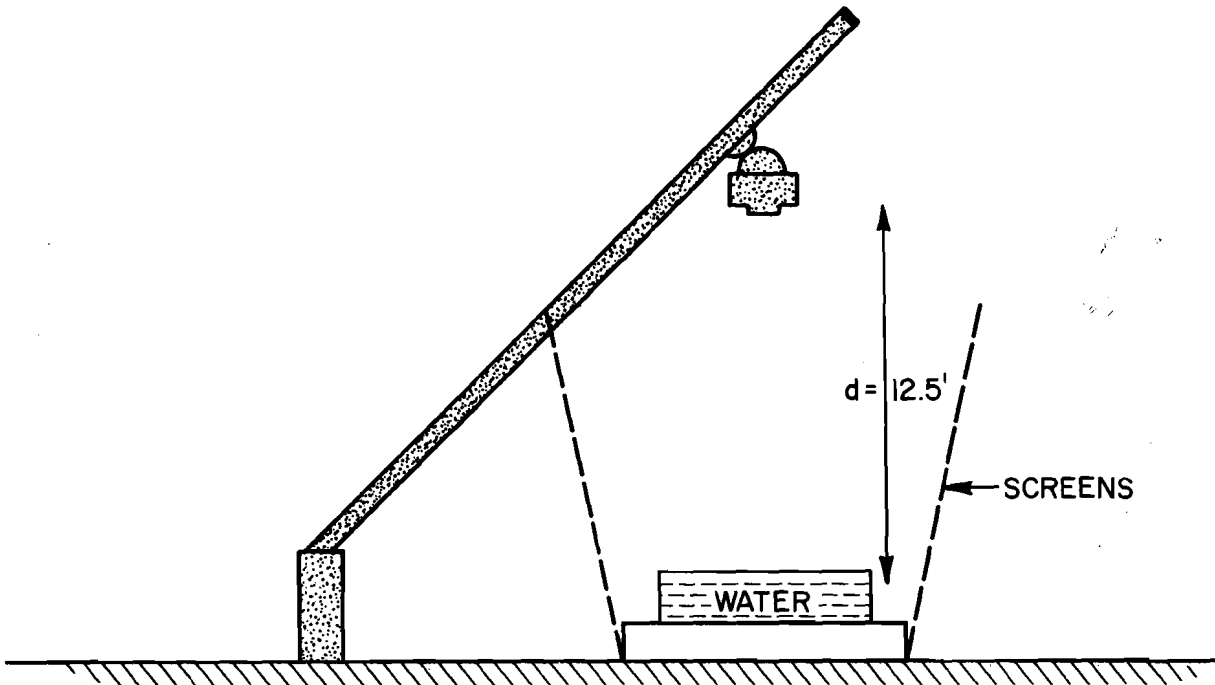


Fig. 2 - Experimental setup for X-band measurements.

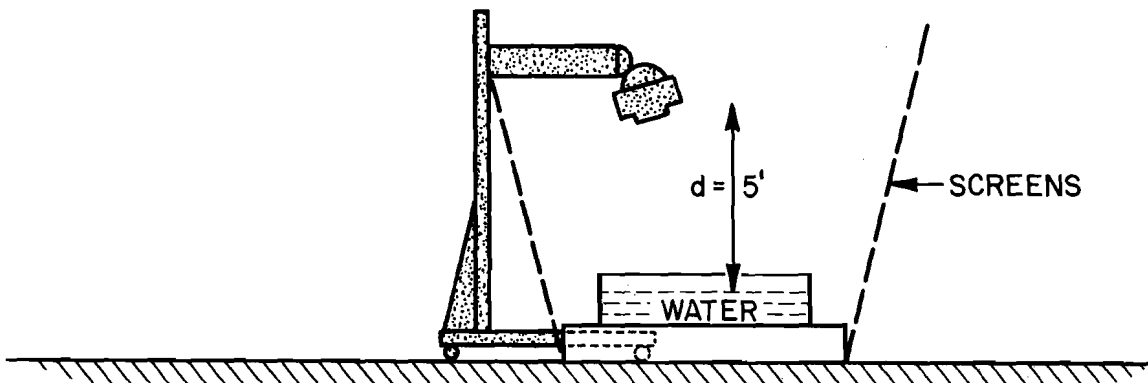


Fig. 3 - Experimental setup for K-band measurements.



Fig. 4 - Foam generator

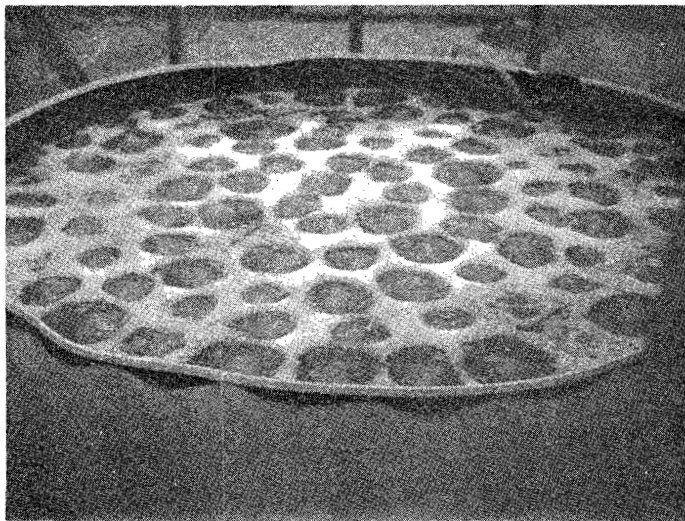


Fig. 5 - Foam pattern at flow rate of $6 \text{ ft}^3 / \text{min}$.

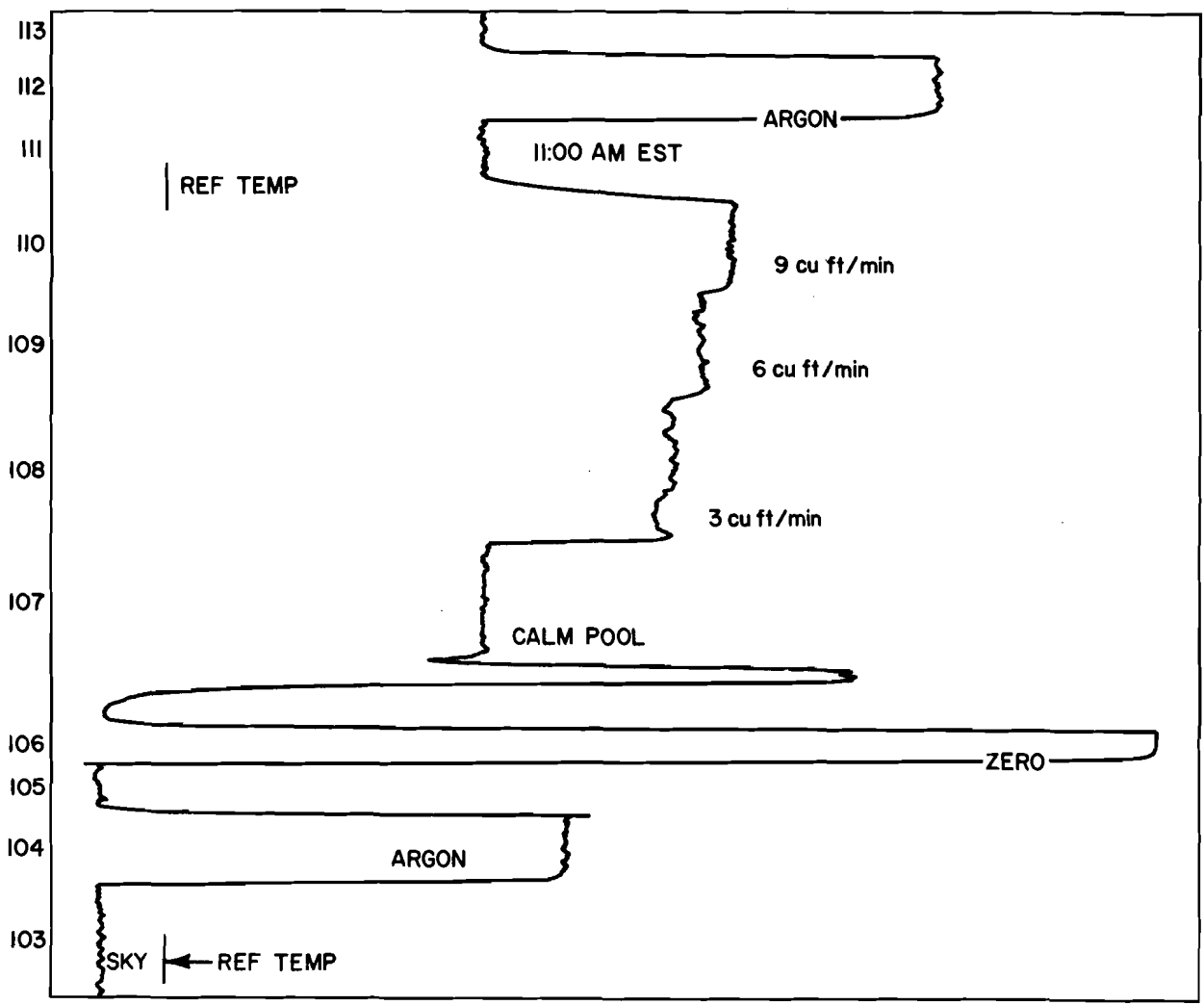


Fig. 6 - Strip-chart record of typical measurement sequence; $\nu = 8.35$ GHz, horizontal polarization, $\theta = 25^\circ$, Jan. 22, 1971.

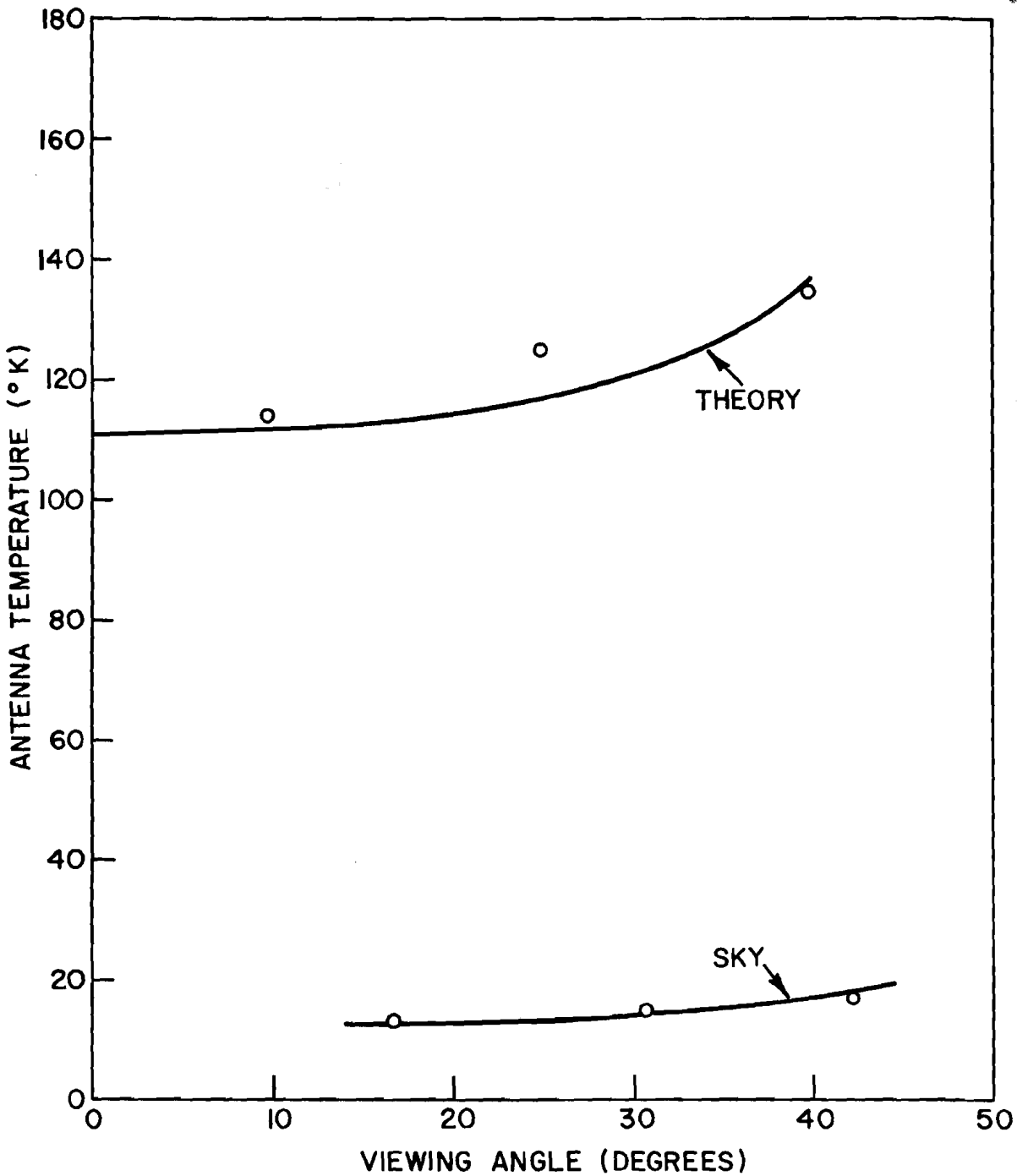


Fig. 7 - Antenna temperature vs angle for calm pool and sky; $\nu = 8.35$ GHz, vertical polarization, Jan. 21, 1971.

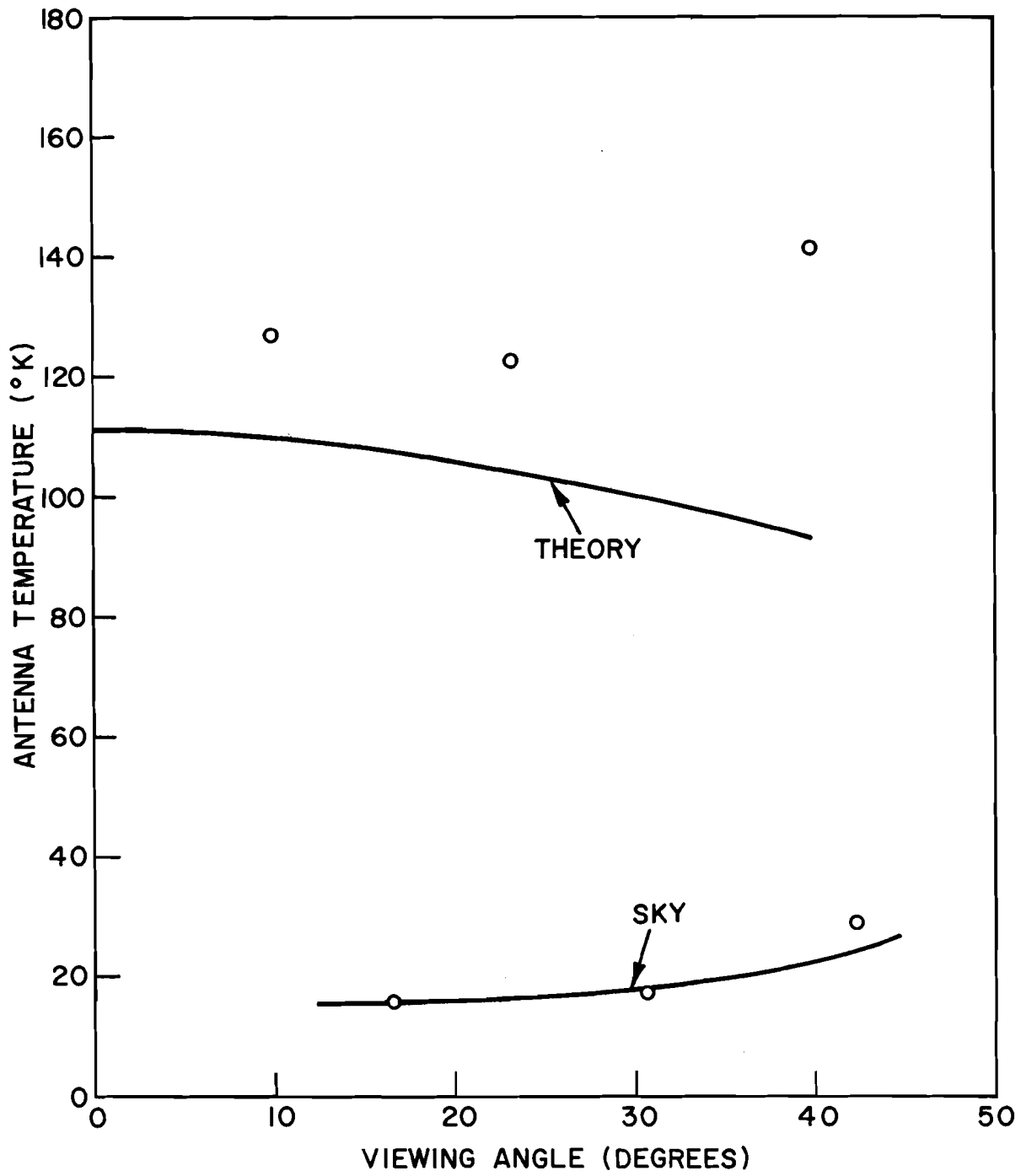


Fig. 8 - Antenna temperature vs angle for calm pool and sky; $\nu = 8.35$ GHz, horizontal polarization, Jan. 21, 1971.

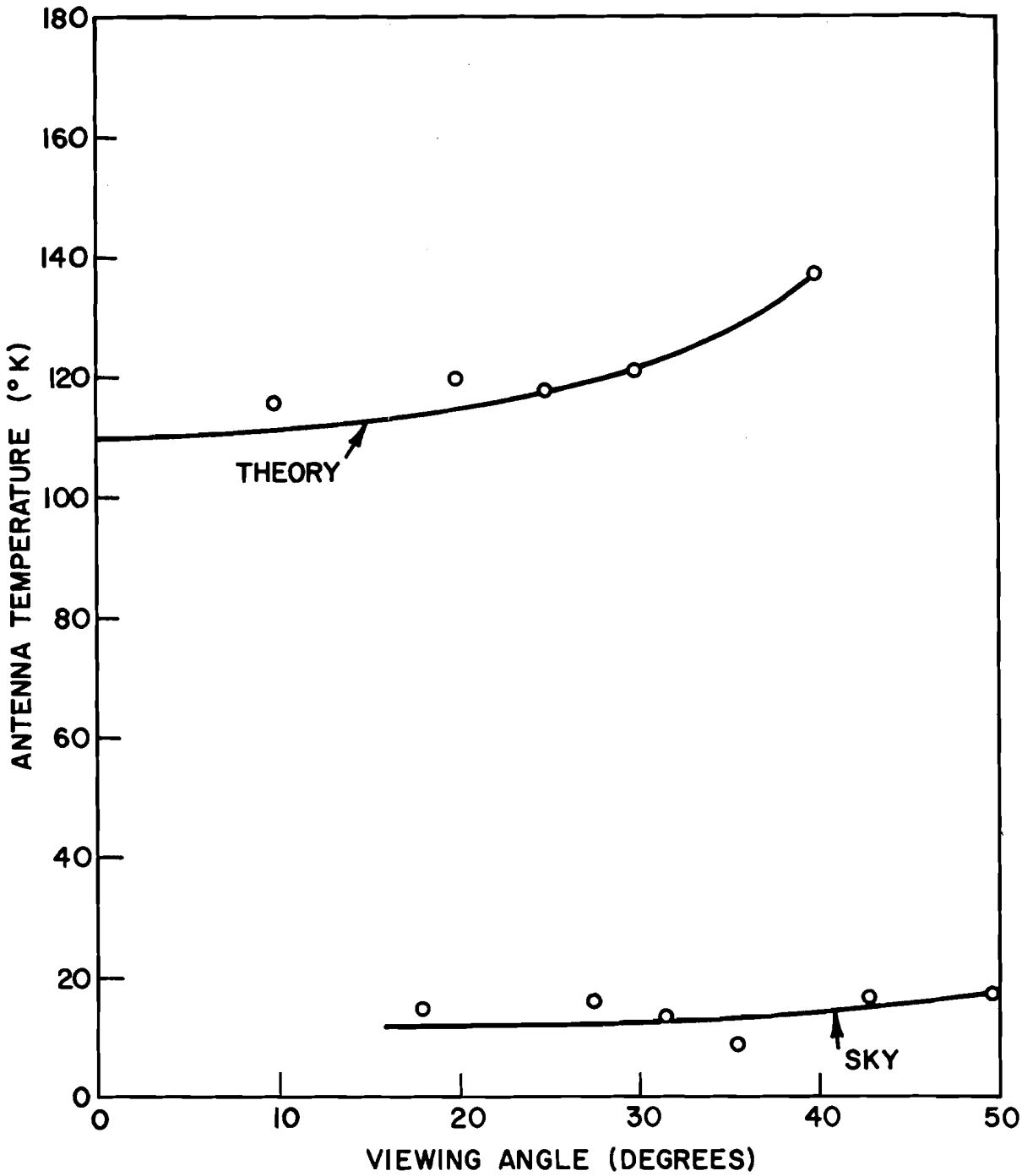


Fig. 9 - Antenna temperature vs viewing angle for calm pool and sky;
 $\nu = 8.35$ GHz, vertical polarization, Jan. 22, 1971.

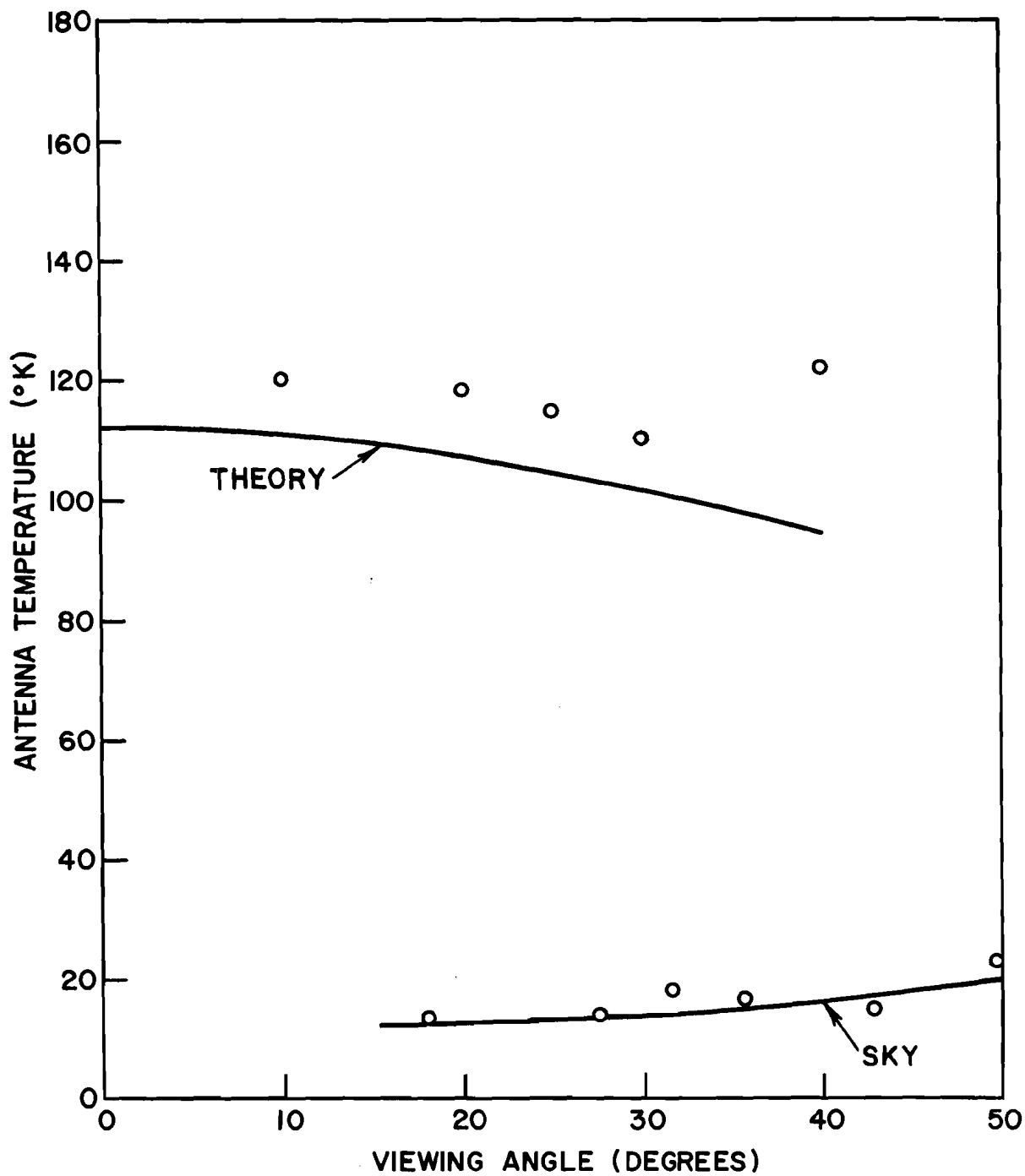


Fig. 10 - Antenna temperature vs viewing angle for calm pool and sky;
 $\nu = 8.35$ GHz, horizontal polarization, Jan. 22, 1971.

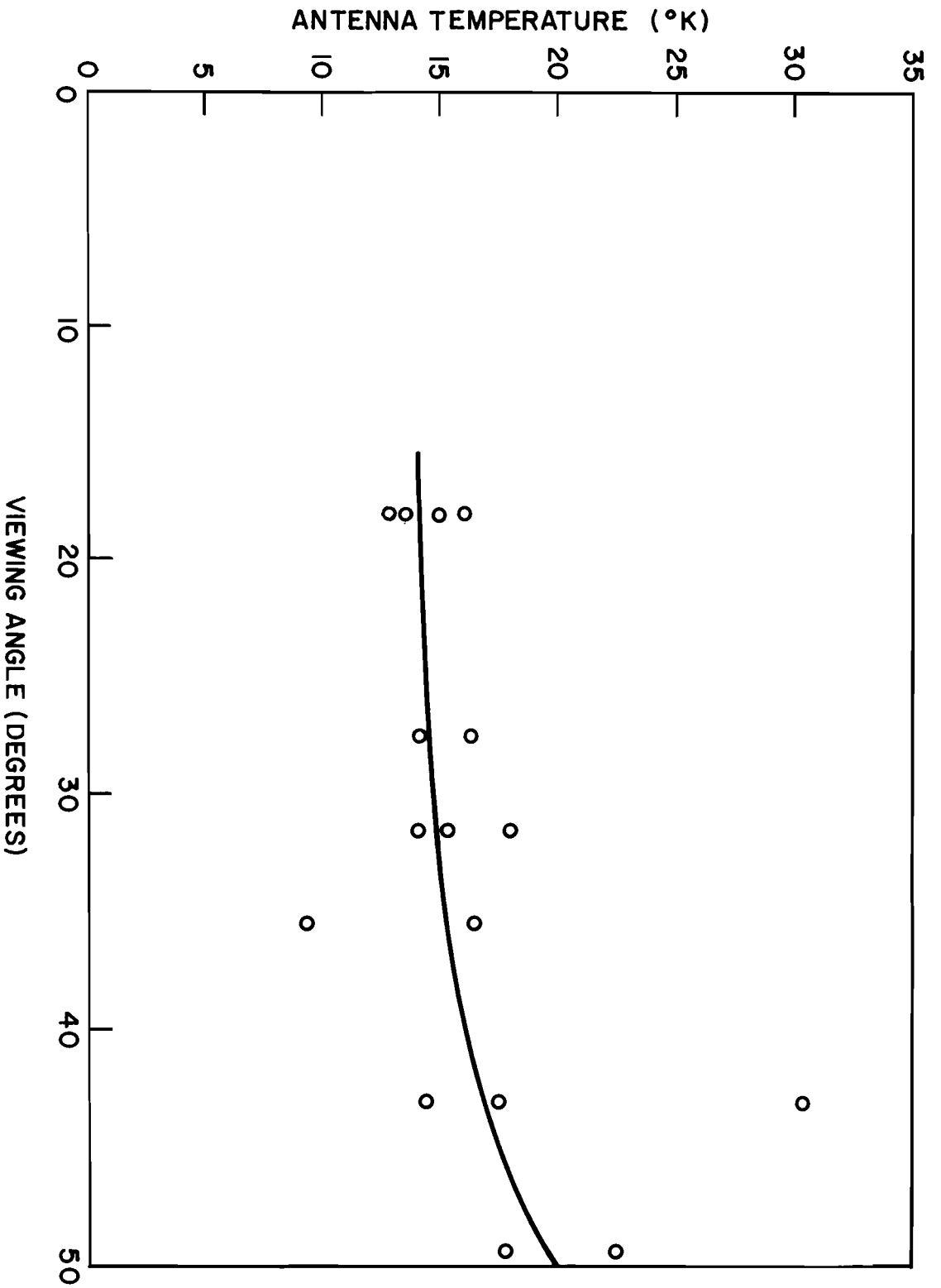


Fig. 11 - Sky temperature vs zenith angle for both polarizations, Jan. 21 and 22, 1971.

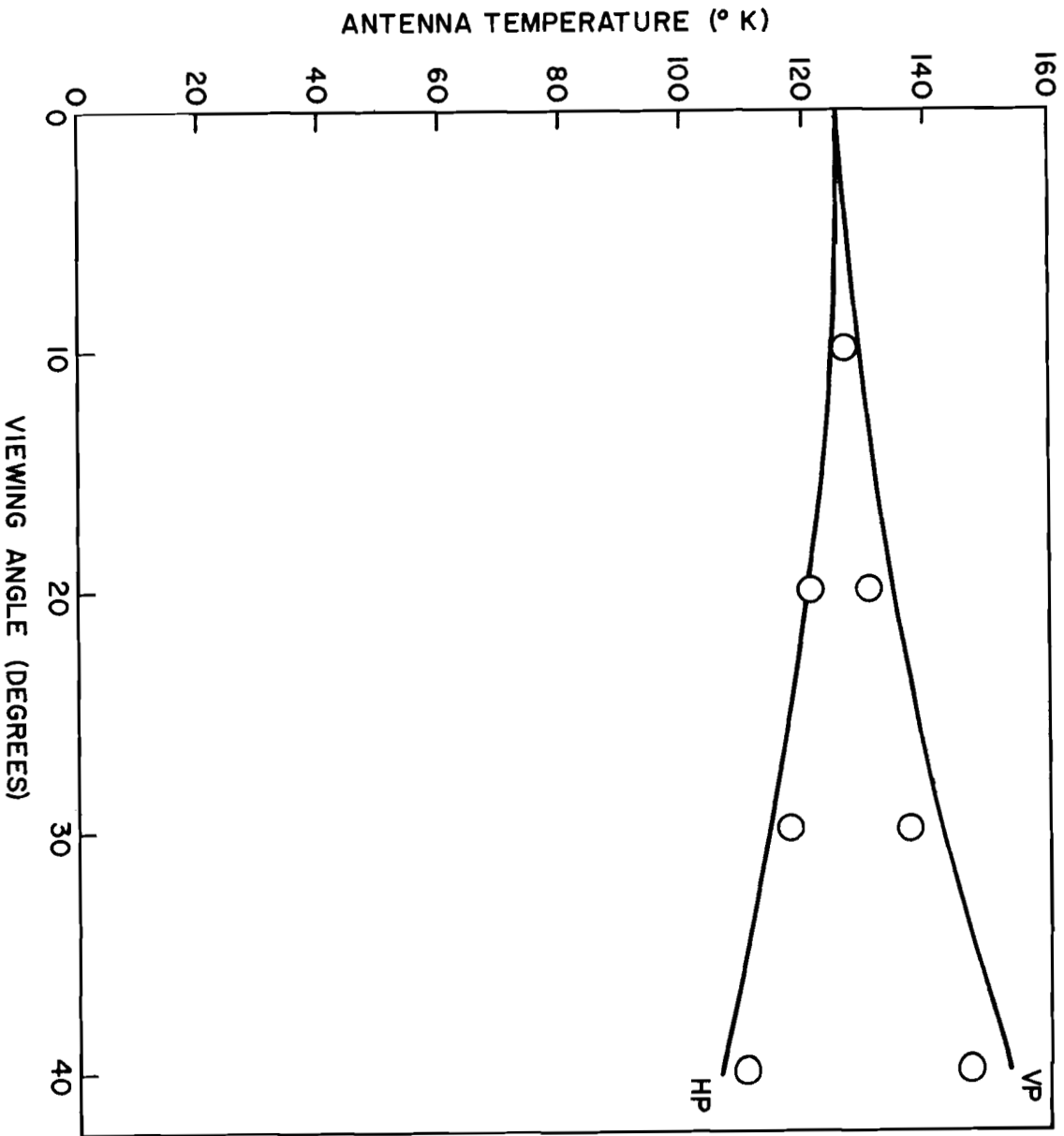


Fig. 12 - Antenna temperature vs viewing angle for both polarizations;
 $\nu = 19.35$ GHz, Jan. 22, 1971.

~~CONFIDENTIAL~~

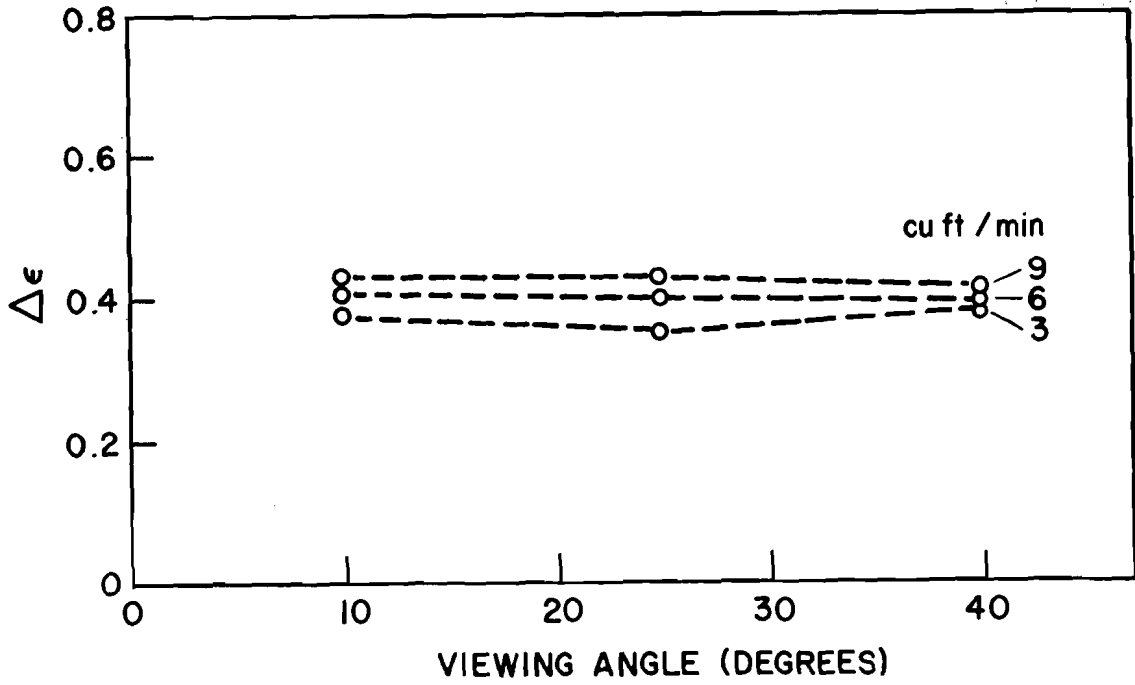


Fig. 13 - Change in emissivity $\Delta\epsilon$ vs angle for horizontal polarization;
 $\nu = 8.35$ GHz, Jan. 21, 1971.

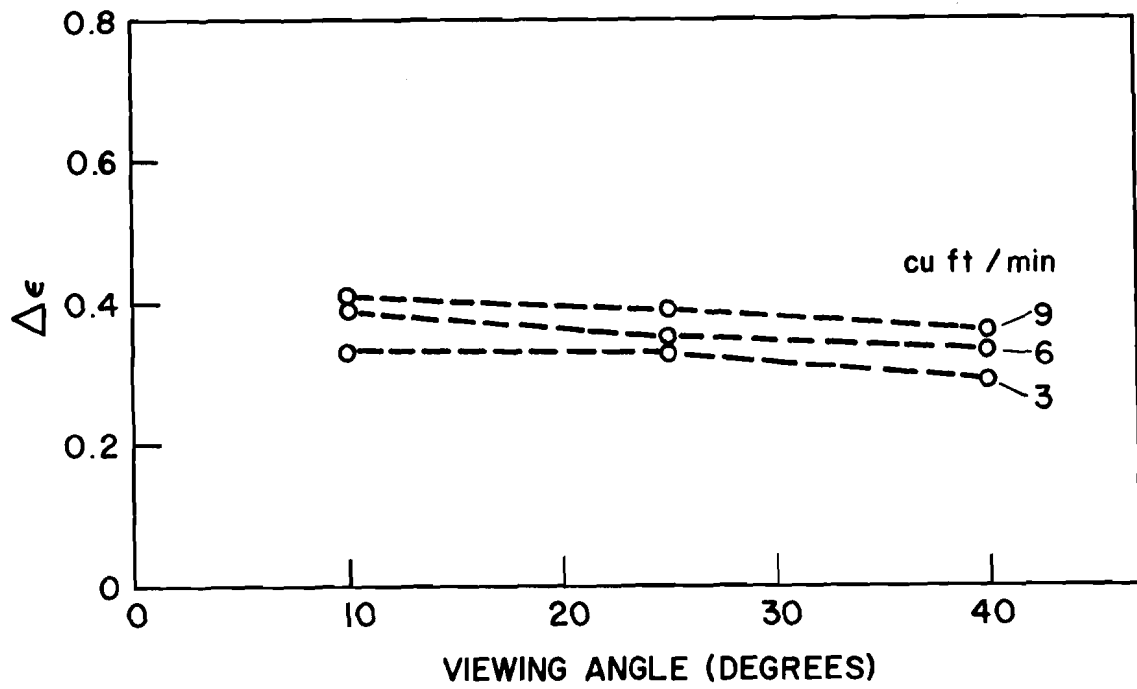


Fig. 14 - Change in emissivity $\Delta\epsilon$ vs angle for vertical polarization;
 $\nu = 8.35$ GHz, Jan. 21, 1971.

~~CONFIDENTIAL~~

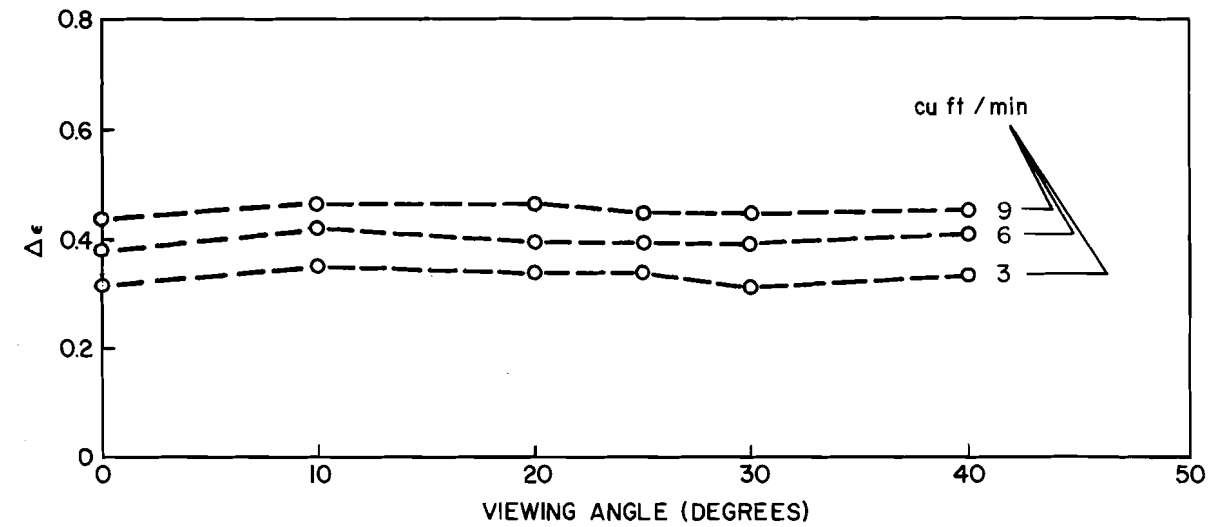


Fig. 15 - Change in emissivity $\Delta\epsilon$ vs angle for horizontal polarization;
 $\nu = 8.35$ GHz, Jan. 22, 1971.

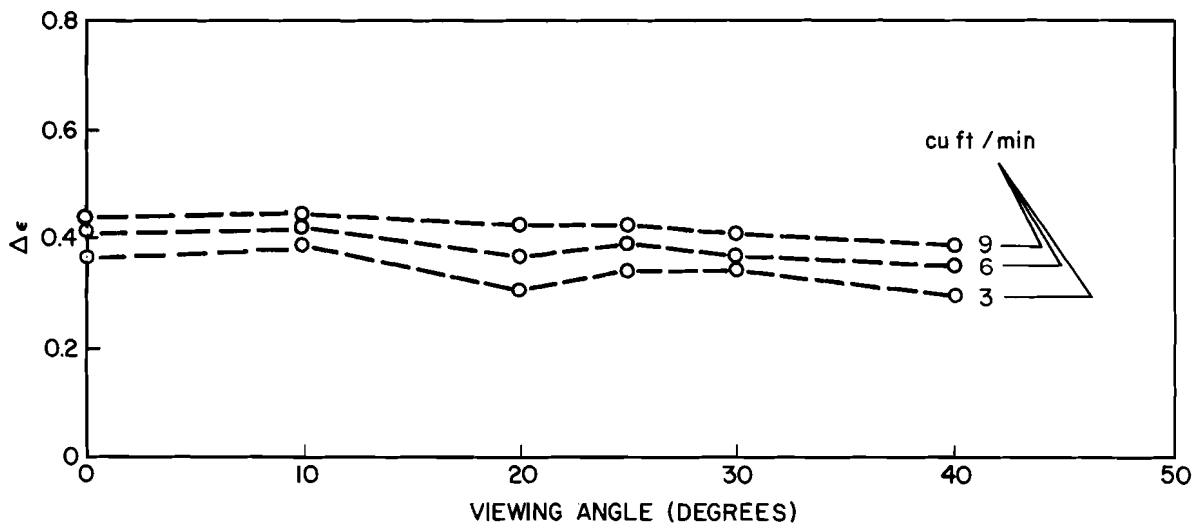


Fig. 16 - Change in emissivity $\Delta\epsilon$ vs angle for vertical polarization;
 $\nu = 8.35$ GHz, Jan. 22, 1971.

CONFIDENTIAL

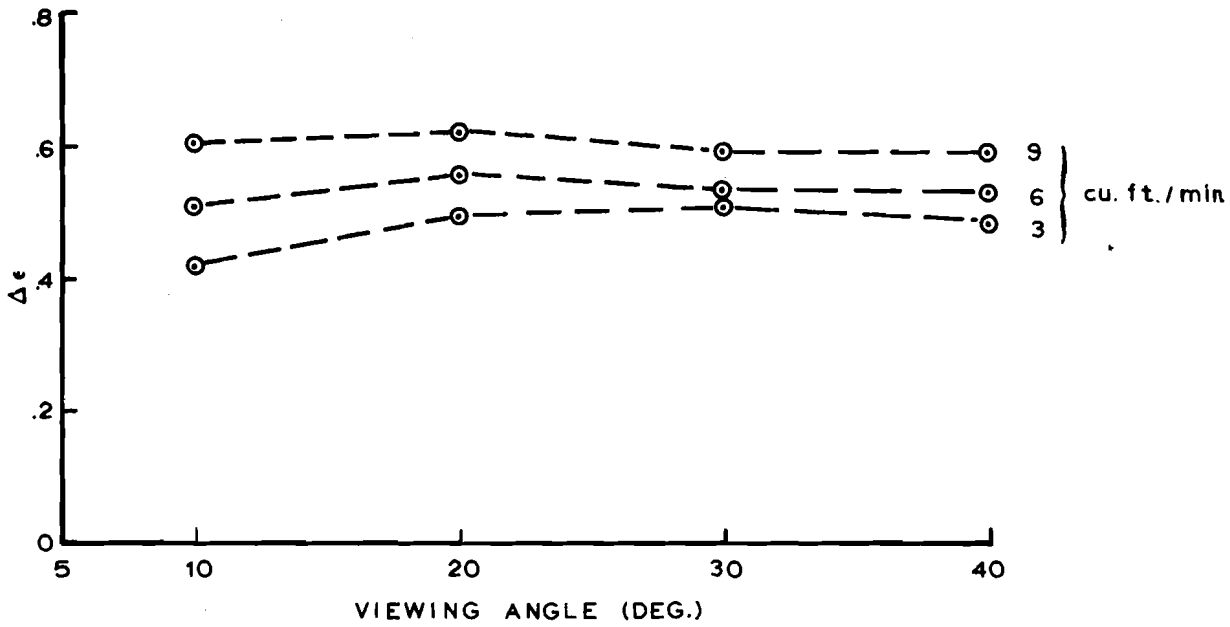


Fig. 17 - Change in emissivity $\Delta\epsilon$ vs angle for horizontal polarization;
 $\nu = 19.35$ GHz, Jan. 22, 1971.

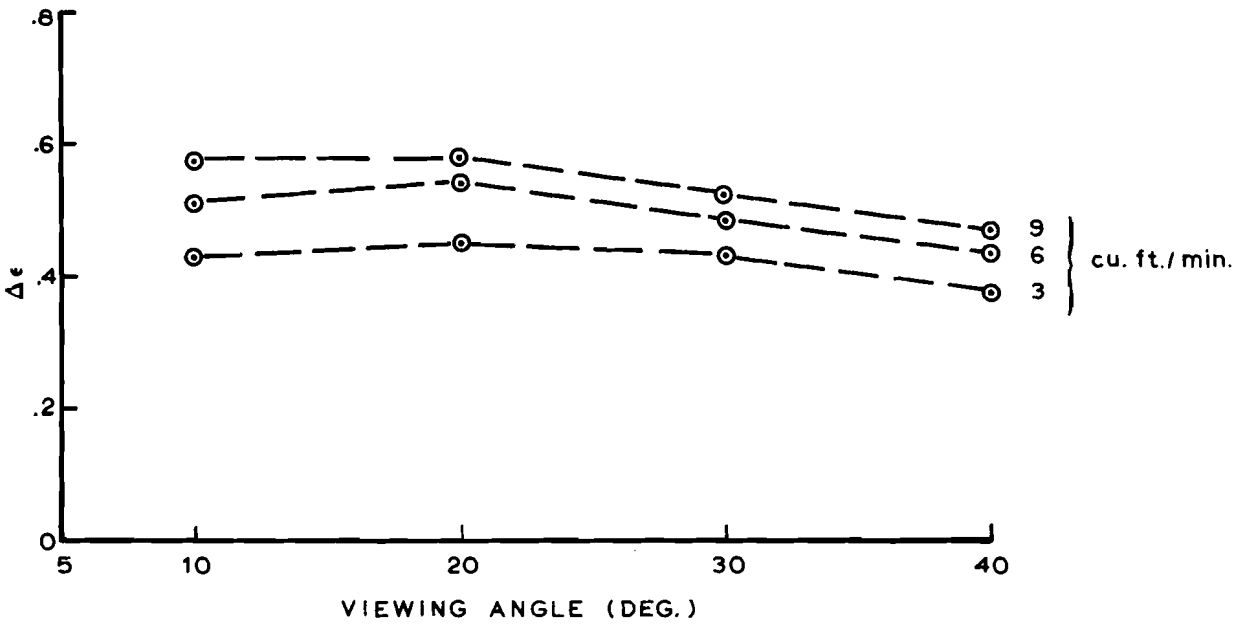


Fig. 18 - Change in emissivity $\Delta\epsilon$ vs angle for vertical polarization;
 $\nu = 19.35$ GHz, Jan. 22, 1971.

~~CONFIDENTIAL~~

Security Classification

DOCUMENT CONTROL DATA - R & D

(Security classification of title, body of abstract and indexing annotation must be entered when the overall report is classified)

1. ORIGINATING ACTIVITY (Corporate author) Naval Research Laboratory Washington, D.C. 20390	2a. REPORT SECURITY CLASSIFICATION CONFIDENTIAL 2b. GROUP 3
---	---

3. REPORT TITLE

THE MICROWAVE EMISSIVITY OF FOAM ON A WATER SURFACE (U)

4. DESCRIPTIVE NOTES (Type of report and inclusive dates)
An interim report on one phase, work continues on this and on other phases.

5. AUTHOR(S) (First name, middle initial, last name)

Lee U. Martin

6. REPORT DATE August 1972	7a. TOTAL NO. OF PAGES 40	7b. NO. OF REFS 6
-------------------------------	------------------------------	----------------------

8a. CONTRACT OR GRANT NO. NRL Problem R02-67A b. PROJECT NO. PM-16-40058C2W44150000 c. d.	9a. ORIGINATOR'S REPORT NUMBER(S) NRL Memorandum Report 2467 9b. OTHER REPORT NO(S) (Any other numbers that may be assigned this report)
--	--

10. DISTRIBUTION STATEMENT
Distribution limited to U.S. Government Agencies only; test and evaluation; August 1972.
Other requests for this document must be referred to the Director, Naval Research Laboratory, Washington, D.C. 20390.

11. SUPPLEMENTARY NOTES	12. SPONSORING MILITARY ACTIVITY Department of the Navy (Naval Air Systems Command) Washington, D.C. 20360
-------------------------	---

13. ABSTRACT

(C) The increase in the microwave emissivity of a foamy water surface over that of a smooth water surface for various viewing angles has been measured under controlled conditions. Measurements were made at frequencies of 8.35 and 19.35 GHz and for both horizontal and vertical polarizations. The change in emmissivity $\Delta\epsilon$ was less at 8.35 GHz than at 19.35 GHz for both polarizations. The angular variation of $\Delta\epsilon$ was smaller with horizontal polarization than with vertical polarization for the frequencies investigated. Experimental results are used to draw tentative conclusions about the detection of ship wakes with microwave radiometers.

14. KEY WORDS	LINK A		LINK B		LINK C	
	ROLE	WT	ROLE	WT	ROLE	WT
Microwave radiometry Foam emissivity Remote sensing						